JOURNAL OF GEOPHYSICAL RESEARCH, VOL. 86, NO. C1, PAGES 429–438, JANUARY 20, 1981

The Damping of Ocean Surface Waves by a Monomolecular Film Measured by Wave Staffs and Microwave Radars

HEINRICH HÜHNERFUSS,[1] WERNER ALPERS,[2] W. LINWOOD JONES,[3] PHILIPP A. LANGE,[4] AND KARL RICHTER[5]

The damping of ocean surface waves by a monomolecular oleyl alcohol film of about 1.5–3 km^2 in area is measured in the North Sea by wave staffs, a coherent X band microwave scatterometer mounted on a sea-based platform, and an incoherent K_u band microwave scatterometer carried by an aircraft under moderate wind conditions (wind speed u_{10} = 3.5–7.7 m s^{-1}). The observed wave attenuation by the monomolecular surface film measured by a wave staff in the frequency band between 3.2 and 16 Hz is in the range of about 40–60%, with only a slight increase with frequency. From this result it can be predicted that slicks affect microwave backscattering similarly in the L band ($\lambda_0 \approx 20$ cm) as in the K_u and X bands ($\lambda_0 \approx 2$ cm). It is shown by additional wave tank experiments that a direct influence of oleyl alcohol surface films on wave damping is confined to frequencies $f \geq 2$ Hz, but a further indirect effect of oleyl alcohol films on the damping of ocean waves in the frequency range between 0.12 and 0.7 Hz by modifying the wind input and wave-wave interaction mechanisms is indicated from our results. A possible directional dependence of the wave-damping effect caused by surface films is discussed.

1. INTRODUCTION

It is well known that monomolecular surface films ('slicks') of biogenic origin cover large areas of the ocean surface and are very predominant in coastal zones [*Barger et al.*, 1974; *Brockmann et al.*, 1976; *Hühnerfuss et al.*, 1977]. These natural slicks strongly affect the surface wave field and thereby influence most air-sea interaction processes, for example, the transfer of energy and momentum from the wind to the wave field [*Barger et al.*, 1970; *Mallinger and Mickelson*, 1973] and the gas exchange at the air-sea interface [*Broecker et al.*, 1978].

The modification of these processes by surface films also has implications for the use of remote sensing techniques in oceanography. For example, the electromagnetic emission in the visible and microwave spectral bands as well as the scattering of these electromagnetic waves is influenced by the presence of monomolecular films [*Au et al.*, 1974; *Cox and Munk*, 1955; *Hühnerfuss et al.*, 1978].

In this paper we report on open ocean and wave tank experiments carried out with the aim of studying the damping of capillary and gravity waves by a monomolecular film. The film material used in our experiments is oleyl alcohol (9-octadecen-1-ol, cis isomer). This material is chosen because it resembles natural slicks in its physicochemical behavior. The decrease in surface tension caused by this surface-active material and that caused by natural slicks are of the same order of magnitude. The same holds for the surface elasticity of both materials [*Garrett*, 1967].

The experiments on the ocean were carried out during the 1975 Joint North Sea Wave Project (Jonswap 75). The wave measurements were performed with resistance wave staffs, a coherent X band microwave scatterometer mounted on a sea-based platform approximately 10 m above mean sea level, and an incoherent K_u band scatterometer carried by an aircraft. In the wave tank, plunger-generated waves were measured with resistance wave gauges.

The main aim of these experiments was to investigate the frequency range over which surface waves are dampened by monomolecular surface films on the open ocean. There is some controversy in the literature concerning this question, *Gottifredi and Jameson* [1968] stated that the wave-damping effect of slicks is confined to short waves with frequencies of $\geq$1.25 Hz ($L \leq 1$ m). In contrast to this, *Barger et al.* [1970] found a significant energy decrease of about 50% in the wave spectrum between 0.4 and 1.0 Hz (L = 9.75–1.56 m).

Since some of the wave-wave interaction mechanisms are supposed to be modified by monomolecular films, another goal of this experiment was to clarify the controversial question of whether the hydrodynamic interaction leads to an energy transfer from the short to the long waves or vice versa.

Another motivation for this experiment was to predict the sensitivity of L band radars to monomolecular surface films. It is well known that microwave backscatter at the rough ocean surface for electromagnetic wavelengths $\lambda_0 \leq 3$ cm and at oblique incidence angles is strongly reduced when the sea surface is covered with a monomolecular film [*Hühnerfuss et al.*, 1978]. The decrease in the cross section is of the order of 5–8 dB. However, it has often been questioned whether L band radar systems, like the system flown on Seasat 1, are as sensitive to slicks as X band or K_u band radars. The Seasat synthetic aperture radar (SAR), which operates at an electromagnetic wavelength of λ_0 = 23.6 cm, views the sea surface with an incidence angle of 20°, and thus the microwave backscattering is due to surface waves with a wavelength of L = 34.5 cm (Bragg wavelength). It is therefore of some interest to know to what extent these surface waves are damped by a monomolecular film.

In the case of experiments on the open sea the observed wave damping by surface films is due to the sum of three processes which cannot be separated: direct influence of the surface film (viscous damping), modification of wind input, and modification of wave-wave interaction. Therefore a comparison of experimental results with theory is relatively restrictive. For this reason we carried out additional wind wave tank experiments with the aim of measuring the attenuation

[1] Institut für Organische Chemie und Biochemie, Universität Hamburg, 2000 Hamburg 13, Federal Republic of Germany.
[2] Institut für Geophysik der Universität Hamburg und Max-Planck-Institut für Meteorologie, 2000 Hamburg 13, Federal Republic of Germany.
[3] NASA Langley Research Center, Hampton, Virginia 23665.
[4] Bundesanstalt für Wasserbau, 2000 Hamburg 56, Federal Republic of Germany.
[5] Deutsches Hydrographisches Institut, 2000 Hamburg 4, Federal Republic of Germany.

Paper number 80C0986.
0148-0227/81/080C-0986$01.00

coefficients for wave damping by a monomolecular oleyl alcohol film in the short gravity wave range excluding effects of changes in the wind input and of wave-wave interaction processes by the film. Thus these measurements can be compared directly with theory.

2. THEORY

It has been well known even since ancient times [*Plinius,* 77 A.D.] that small quantities of oil poured on the ocean surface damp short ripple waves. But until now it was not fully understood which physical mechanisms cause this wave damping.

One mechanism leading to wave damping in the presence of surface slicks is described by *Phillips* [1977]. Owing to a different boundary condition at the surface, the flow in the boundary layer changes, which leads to enhanced wave attenuation.

The energy dissipation of wave energy in water not contaminated by a surface film is given by

$$\dot{E} = E_0 \cdot e^{-2\gamma_\nu t} \tag{1}$$

with the attenuation coefficient

$$\gamma_\nu = 2 \cdot \nu \cdot k^2 \tag{2}$$

where $\nu = \mu/\zeta$ is the kinematic viscosity of the water and k the wave number of the water wave.

However, in the presence of a densely packed surface film ('inextensible' film according to Phillips), which is practically incompressible to tangential stresses, one obtains in deep water for the attenuation coefficient

$$\gamma_f = \tfrac{1}{2}\nu\beta k \tag{3}$$

where β is given by [see *Phillips,* 1977]

$$\beta = (\omega/2\nu)^{1/2} = (\tfrac{1}{2}R_w)^{1/2} \cdot k \tag{4}$$

(ω is the frequency of the wave, and R_w the wave Reynolds number). Except for very short capillary waves we have

$$\gamma_f/\gamma_\nu = \tfrac{1}{4}\beta \gg 1 \tag{5}$$

According to this theory the attenuation coefficient (3) is independent of the chemical character of the surface film. However, a monomolecular surface film in general is not inextensible; it has a finite surface elasticity which depends on the chemical structure of the monomolecular film. One expects that a finite elasticity of the surface film leads to a higher attenuation coefficient than that given by (3).

Several authors (for reviews, see *Davies and Rideal* [1963]) performed experiments with mechanically generated waves in the high-frequency capillary range ($f \geq 50$ Hz) and proved a dependence of the damping on the surface-active compound. In connection with those experiments a theoretical treatment of the damping effect has been published considering energy dissipation occurring only by viscosity effects within the film itself [*Bendure and Hansen,* 1967; *Goodrich,* 1961, 1962; *Lucassen and Hansen,* 1966; *van den Tempel and van de Riet,* 1965]. Another group of authors tried to take into account the physical processes occurring in a bulk water/monolayer system during passage of a wave, too [*Drost-Hansen,* 1972; *Garrett and Zisman,* 1970; *Horne,* 1972; *Vollhardt and Wüstneck,* 1978].

Nearly all laboratory experiments and theories cited above dealing with the study of molecular interactions between film molecules and bulk water as a main cause for wave damping are confined to relatively high frequency water waves ($f \geq 50$ Hz).

However, in the open ocean, lower-frequency water waves are also observed to be affected by the surface film, as will be shown in this paper. It has to be investigated whether the observed wave damping can be explained by the mechanism described by *Phillips* [1977] or whether other mechanisms contribute to wave damping as well.

3. SLICK EXPERIMENTS

a. *North Sea Experiments*

During the Joint North Sea Wave Project 1975, several artificial monomolecular surface films of oleyl alcohol were produced in the North Sea off the island of Sylt. The method [*Hühnerfuss and Lange,* 1975] involved a systematic dissemination of frozen chunks (80 g) of 96.5% pure oleyl alcohol (9-octadecen-1-ol, cis isomer) from a helicopter. Under the influence of this surface-active material the surface tension decreased from the normal value of about 74 dyn/cm to about 43 dyn/cm. These values were obtained by in situ measurements using the spreading oil method developed by *Adam* [1937].

Here we report the results of three slick experiments performed on September 3 (slick 2), September 4 (slick 1), and September 10 (slick 3), 1975 (see Table 1), during which the slick drifted toward the research tower Pisa (54°59′42″N, 7°54′22″E), located 27 km offshore on the Jonswap profile [*Hasselmann et al.,* 1973]. The slicks were produced at a distance of about 1 km from station Pisa such that wind and wave fields at this measurement site were not disturbed. In order to have the slicks drift toward Pisa a careful study of wind, current, and wave direction was necessary in each case. The method used for predicting the slick drift is described by *Lange and Hühnerfuss* [1978]. The size of the slicks varied between 1×1.5 km^2 and 1.5×2 km^2.

Wave measurements were performed inside and outside the slick area while the slick drifted by. The wave measurements at the station Pisa were performed by two resistance wave staffs and by a microwave scatterometer.

The experimental configuration is shown in Figure 1. One wave staff, here called the 'vertical' wave staff, was capable of measuring the long as well as the short (capillary) waves. Since the principal goal of the tower experiment was the study of the hydrodynamic modulation of the short waves by the long waves, the output of the vertical wave staff was both low- and high-pass-filtered to yield the low-frequency and high-frequency parts of the one-dimensional surface wave spectrum. The output of the low-pass and high-pass filters contains waves in the frequency range 0–0.7 Hz and 3.6–16 Hz, respectively. The upper limit of 16 Hz was determined by the time required for water to drain from the probe surface. This seems to prohibit capillary wave measurements with resistance wave staffs for higher frequencies [see *Tober et al.,* 1973].

The other wave staff, here called the 'oblique' wave staff, was capable of measuring only the low-frequency part (0–0.7 Hz) of the one-dimensional surface wave spectrum.

The microwave scatterometer was a coherent Doppler radar operating at an electromagnetic wavelength of 3.16 cm (*X* band). The antenna of the scatterometer was mounted on an outrigger of Pisa approximately 10 m above sea level (see Figure 1) and could be rotated in azimuth by 270° and in eleva-

TABLE 1. Date, Time, and Experimental Parameters of the Three Slick Experiments and the Available Data From Wave Staffs and Microwave Sensors

	Date, 1975	Local Time	Wind Direction at Pisa	Wind Speed at Pisa, m s^{-1}	Significant Wave Height at Pisa, m	Frequency at Swell Peak, Hz	Frequency at Wave Peak, Hz	Data Sources
Slick 1	Sept. 4	0813–0920	295°–311°	3.5–7.7	1.4	0.1	0.2	wave staffs AAFE radscat
Slick 2	Sept. 3	1518–1546	310°	3.6–4.1	0.6	0.1	0.45	wave staffs
Slick 3	Sept. 10	1724–1925	228°	6	1.6	0.1 (weak)	0.35	wave staffs tower scatterometer (backscattered power and Doppler shift)

tion between 30° and 70° incidence angle. The half-power beam width of the antenna was 5°, such that an elliptical area of about 1.2 × 1.8 m^2 was illuminated on the surface for 45° incidence. The backscattered microwave power P as well as the Doppler frequency shift f_d was measured as a function of time [see *Wentz and Jones,* 1976].

Wave measurements were obtained by using wave staffs at Pisa for the three different slick events; however, the scatterometer was operating only at event 3 (slick 3) on September 10, 1975. In addition, during event 1 (slick 1) the slick area was overflown by the NASA C-130 aircraft carrying a 13.9-GHz pencil beam scatterometer (AAFE radscat).

The environmental parameters of these three experiments are summarized in Table 1.

Slick 3 was produced between 1723 and 1747 MET (middle European time) as a continuous and uniform surface film approximately 1 km southwest of Pisa. The arrival of the slick occurred around 1805 MET, when the mean backscattered power P of the tower scatterometer suddenly decreased by about 6.35 ± 1.87 dB, as is shown in Figure 2. In this plot of relative P versus time each data point represents the average of 32.5 s, and it can be seen that the slick is already broken into patches (streaks) when it arrives at Pisa. Relatively uniform slick areas can be identified in Figure 2 and are labeled $B1$ and $B2$. The times T that it takes the uniform slick patches to drift through the antenna beam are $T_1 = 243$ s and $T_2 = 311$ s, respectively. The corresponding linear dimension D of these slick areas is given by the product of the drift velocity and the times T_i ($i = 1, 2$). Our estimate for D is $D_1 = 200$ m for area $B1$ and $D_2 = 250$ m for area $B2$. The gross structure of slick 3 at Pisa is not known exactly, but on the basis of the radar measurements and visual observations the spatial distribution of the slick can be approximated by the diagram shown in Figure 3*a*. Figure 3*b* shows the geometry of the experiment. The wind vector in Figure 3*b* is measured at the tower Pisa, while the drift velocity for the slick is an estimate based on visual observations and theoretical considerations [see *Lange and Hühnerfuss,* 1978].

The arrival of the slick at the vertical wave staff was also discernable from the decrease in the squared high-pass-filtered output. In Figure 2 we have also inserted the time intervals $B'1$ and $B'2$, during which the slick patches drifted through the location of the vertical wave staff.

In order to study the attenuation of the short waves by monomolecular surface films we calculated the one-dimensional wave spectra in the slick patch $B'1$ and in the slick-free area C from the high-pass-filtered signal of the vertical wave staff. The ratio of the spectra in areas $B'1$ and C, $E_{B'1}/E_C$, is plotted in Figure 4 (frequency range 3.2–16.0 Hz). The scale on the right-hand side of this plot shows the corresponding values for the wave attenuation in percent.

Because the slick patch $B'1$ drifted through the location of the vertical wave staff in $T_1' = 149$ s, the time available for the spectral analysis was relatively short. The parameters used for the spectral analysis are summarized in Table 2.

No values for $E_{B'1}/E_C$ in the frequency ranges 4.1–6.1 and 9.3–13.9 Hz are given, since the spectra showed a resonance-like behavior in these regions on this particular day. This resonance occurred in the slick data as well as in the slick-free data. We believe that it was generated by vibrations of the suspension of the wire. On other days with different wind and wave conditions such a resonance was absent (see slick 1 (Figure 6), and slick 2 (Figure 7)). We feel that the data from these resonant portions of the spectra should be deleted in order not to bias the results.

We have also tried to study the attenuation of the long waves by slick 3 by analyzing the low-pass-filtered signal of the vertical wave staff and the oblique wave staff in the range between 0 and 0.72 Hz. The attenuation measured with the oblique wave staff is shown in Figure 4 (frequency range 0-0.72 Hz).

Simultaneous measurements of the backscattered microwave power P (Table 3) and the Doppler shift f_d (Figure 5) have been carried out with the tower scatterometer. The antenna was pointing at the sea surface with an incidence angle of 57° and an azimuth angle of 258°N (see Figure 3*b*). The scatterometer was operating at horizontal polarizations in both the transmitting and the receiving mode.

The line-of-sight velocity of the illuminated ocean patch is

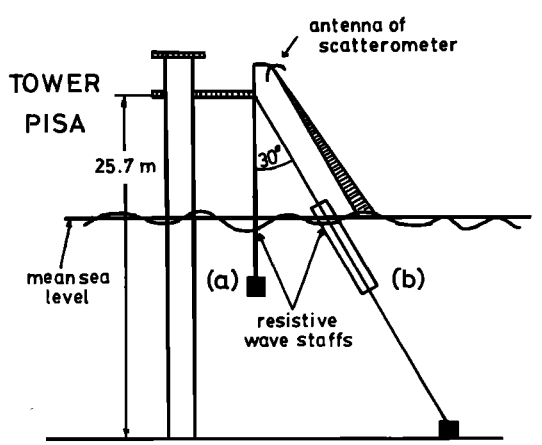

Fig. 1. Experimental configuration of the vertical wave staff (*a*), the oblique wave staff (*b*), and the scatterometer mounted on the sea-based tower Pisa.

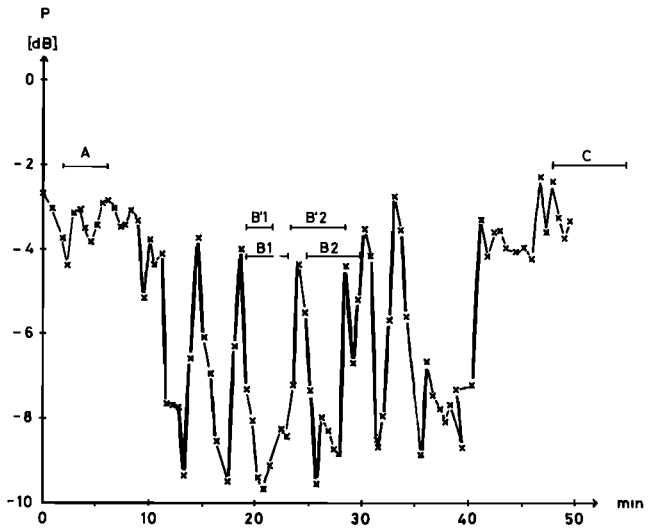

Fig. 2. Relative mean backscattered power P measured by the tower scatterometer versus time during the passage of slick 3. A and C mark the time intervals of the nonslick areas, $B1$ and $B2$ those of the slick areas which have been evaluated for radar measurements, and $B'1$ and $B'2$ those of the slick areas during which wave staff data have been analyzed.

measured by the Doppler shift of the backscattered microwave signal, which is given by

$$f_d = \frac{1}{\pi}\mathbf{K}\cdot(\mathbf{V}_{ph} + \mathbf{U} + \mathbf{V}^c + \mathbf{V}^w + \mathbf{V}^{st})$$

where the dot designates the scalar product, K the electromagnetic wave vector, $\mathbf{V}_{ph}$ the phase velocity of the Bragg scattering wave, U the orbital velocity associated with the long wave, $\mathbf{V}^c$ the current velocity, $\mathbf{V}^w$ the wind drift, and $\mathbf{V}^{st}$ the Stokes drift. Assuming that all velocities except the orbital velocity U are time independent, then the spectrum $f_d(t)$ is directly related to the spectrum of the orbital velocity in the look direction of the antenna. In turn, the orbital velocity is related to the surface elevation associated with the long waves. Thus by measuring the spectrum of the Doppler shift the wave spectrum can be measured. In this sense the coherent microwave scatterometer can be used as a wave probe [*Keller and Wright*, 1975].

The connection between the spectrum of the Doppler shift in wave number space, $P_{fd}(\mathbf{k})$ and the surface elevation spectrum of the long waves in wave number space, $P_\zeta(\mathbf{k})$, is given by

$$P_{fd}(\mathbf{k}) = |\mathbf{K}|^2(\omega/\pi)^2[\sin^2\theta\cos^2\phi + \cos^2\theta]P_\zeta(\mathbf{k})$$

where θ is the incidence angle ($\theta = 0$ for vertical incidence); ϕ the (azimuth) angle, that is, the angle between the look direction of the antenna and the direction of $\mathbf{k}$; and $|\mathbf{K}| = 2\pi/\lambda_0$ the electromagnetic wave number. A derivation of the above formula is given in the appendix.

Transforming this relation to frequency space implies an integration over the angle ϕ. If the slick reduces all components of the two-dimensional surface wave spectrum to an equal amount, then the ratio of the Doppler shift spectra in frequency space for slick-free and slick-covered areas is equal to the corresponding ratio of the surface elevation spectra in frequency space. However, if the damping by the slick is dependent on the wave direction, this is no longer true. Thus we conclude that significant deviations of the damping ratio measured by the wave staff and the Doppler shift may be attributed to directional effects in the damping mechanism.

The experimental conditions during event 1 (slick 1) and event 2 (slick 2) are similar to those, shown in Figures 3*a* and 3*b*, with only slight alterations in wind direction and wind speed as summarized in Table 1. But in these cases neither the visual observations nor the high-pass-filtered signal of the vertical wave staff showed any evidence for a patchy structure of the slicks. Thus a record time of 500 sec for slick data was available, corresponding with a linear dimension of $D = 400$ m for the slick. For a spectral resolution $\Delta f = 0.156$ Hz, 79 spectra could be averaged. The results of slick 1 (Figure 6) and slick 2 (Figure 7) consequently show much smaller error bars than those of slick 3.

The reduction of the microwave backscattering cross section was measured from an aircraft during event 1 (slick 1) at

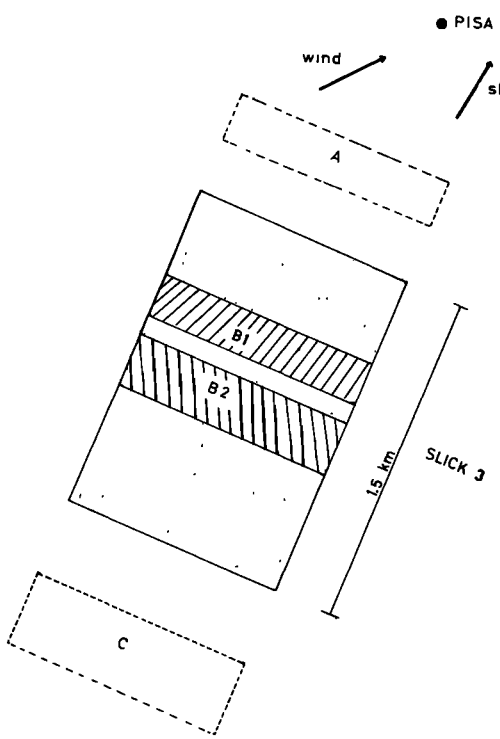

Fig. 3*a*. Spatial distribution of the nonslick areas A and C and the slick areas $B1$ and $B2$ of slick 3.

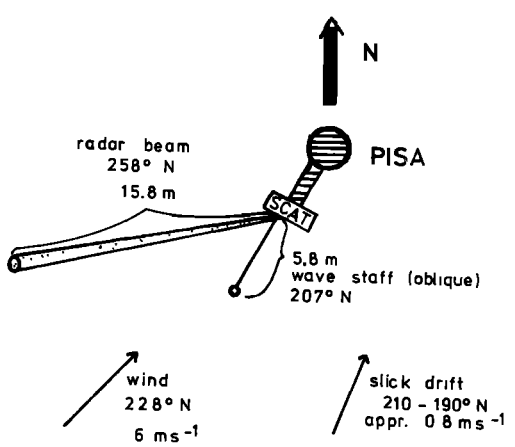

Fig. 3*b*. Geometry of the slick 3 experiment.

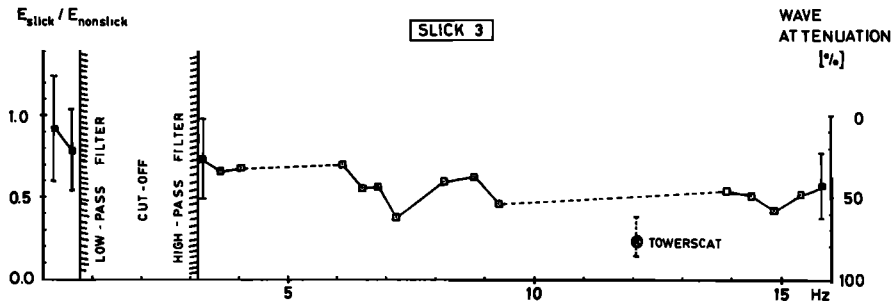

Fig. 4. Ratio of the wave energy of slick area $B'1$ of slick 3 and nonslick area C versus frequency measured by the oblique wave staff (0.12–0.72 Hz) and by the high-pass-filtered signal of the vertical wave staff. The scale on the right-hand side shows the corresponding values for the wave attenuation in percent. The encircled cross marks the value measured by the tower scatterometer. The error bars at the spectral ratios designate 90% confidence limits, while the error bar at the scatterometer data point refers to standard deviation.

incidence angles of 41° and 47°. The results of these measurements have already been reported in detail elsewhere [*Hühnerfuss et al.*, 1978].

b. *Wind Wave Tank Experiments*

In order to separate direct damping effects (viscous damping) of oleyl alcohol surface films from indirect effects (modified wind input and modified wave-wave interaction) we performed some experiments in our wind wave tank [see *Hühnerfuss et al.*, 1976]. Plunger-generated waves of 1, 2, and 2.5 Hz were allowed first to propagate over a carefully cleaned water surface and then over a surface covered with an oleyl alcohol surface film. In the case of the slick experiment the amplitudes of the waves were measured at the beginning of the slick and at distances of 4, 8, and 12 m. Only small-amplitude waves were produced such that the frequency of the waves did not change with travel distance in the wind wave tank. This was controlled by on-line fast Fourier transform analysis of the wave staff outputs. For high amplitudes a broadening of the initially sharp spectral peak occurred at the larger distances, which is attributed to nonlinear interactions, which would bias our data.

The wind generator was turned off in this experiment.

4. Discussion of Results

a. *North Sea Experiments*

For slick 3 (Figure 4) the ratio of the wave spectral energies in the slick area $B'1$ and the slick-free area C (see Figure 2) is measured to lie between 0.38 and 0.73 in the frequency range 3.2–16 Hz. The average value is 0.56 in this frequency range. Though the confidence limits are relatively large because of the short record time, the data clearly show a slight increase of wave attenuation with frequency.

For slick 1 (Figure 6) the average value for the ratio of the spectral energies in slick-covered and non-slick-covered areas is measured to be 0.48 in the frequency range between 3.7 and 16 Hz. No increase of the wave attenuation with frequency is evident from these data on account of the larger scatter of the data points, which vary between 0.17 and 0.83.

For slick 2 (Figure 7) the ratio of the spectral energies varies between 0.84 and 0.18 in the frequency range 3.9–16 Hz, and the average value is 0.44. Again a slight increase of wave attenuation with frequency is discernable.

The wave damping calculated for the low-frequency part of the spectrum (Figures 4, 6, and 7) is less conclusive, but the data seem to indicate that waves in the frequency range between 0.12 and 0.7 are still subject to some damping due to the presence of monomolecular slicks. We expect this damping to be detectable only after the waves have propagated through the slick for a distance of many wavelengths. A further discussion on the damping of gravity waves and a comparison with theory are given in the theoretical part (section 5) of this paper.

The microwave scatterometer measurements which were carried out simultaneously with the wave staff measurements support these results. Backscattering of microwaves on the rough ocean surface at oblique incidence angles (approximately 30°–70°) can be used for measuring short ocean waves [*Wright*, 1966, 1968; *Valenzuela et al.*, 1971]. To first order in wave slope the backscattered power is proportional to the en-

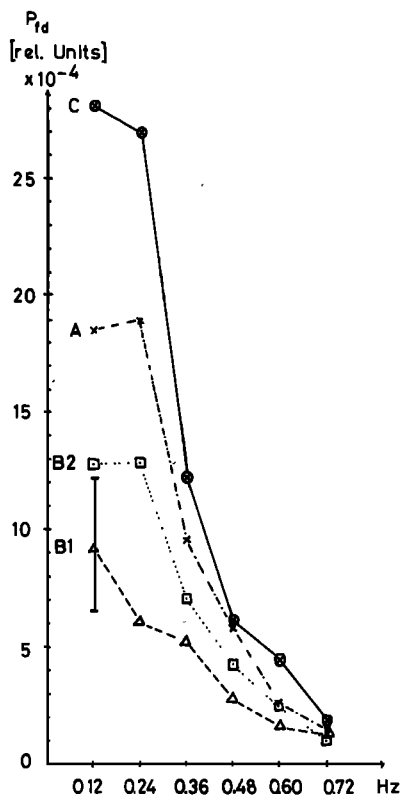

Fig. 5. Spectra of the Doppler shift P_{fd} versus frequency measured during passage of nonslick areas A and C and slick areas $B1$ and $B2$ of slick 3.

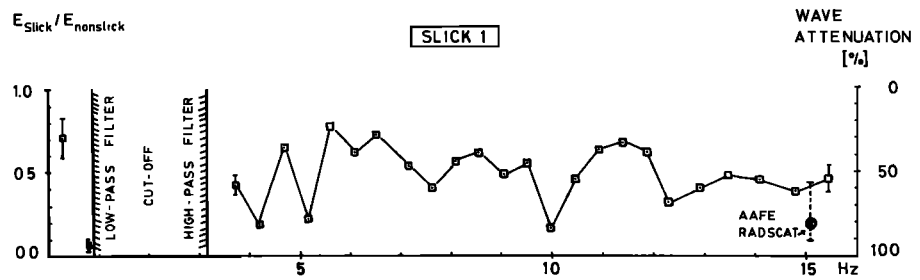

Fig. 6. Ratio of wave energy of slick area of slick 1 and nonslick area versus frequency measured by the vertical wave staff. The scale on the right-hand side shows the corresponding values for the wave attenuation in percent. The encircled cross marks the value measured by the airborne K_u band scatterometer (AAFE radscat).

ergy density of the surface waves at the Bragg wavelength. For first-order scattering this length is given by

$$L = \lambda_0/(2 \sin \Theta)$$

where λ_0 is the free space radar wavelength and Θ the incidence angle measured with respect to the normal to the mean surface. Further, unlike the wave staff, which measures the spectral energy averaged over all azimuthal directions, $P(L)_{avg}$, the scatterometer measures only the component of spectral energy in the radar look direction, $P(L, \psi)$, where ψ is the azimuth angle between the radar and the spectral peak (upwind) direction. Therefore the relative change in backscattered power due to the surface films is equal to the relative change in the directional wave spectral energy at this particular wavelength.

In the case of slick 3 the change in backscattered power measured by the tower scatterometer was 6.35 ± 1.87 dB. This means that the spectral energy at the water wavelength L = 1.88 cm, corresponding to a frequency of 12.2 Hz, decreased by 77%. This value is inserted in Figure 4. This value is lower than the one measured by the wave staff (about 50%), but because of the large error bars it is still consistent with the wave staff measurements.

Another possible explanation for the difference between the scatterometer and wavestaff measurements may be found by examining the directional characteristics of the capillary spectrum. When generated by the wind, the capillary spectrum has the form $P(L, \psi) = P(L)_{avg}(1 + 0.6 \cos 2\psi)$ [*Jones et al.*, 1978]. It is possible that the presence of the slick modifies this anisotropy and that the spectrum becomes more isotropic. For slick 3, $\psi = 30°$, so that $P(1.88, 30°) = 1.35(L)_{avg}$; therefore if the energy were redistributed in direction to form an isotropic spectrum, then the energy at $\psi = 30°$ would be reduced. If one assumes that the wave staff measures the $P(1.88) = 77\%$, then the scatterometer should have measured 59% for the isotropic case.

During event 1 (slick 1) the decrease in backscattered power measured by the airborne microwave scatterometer is 7.3 ± 3.5 dB at 47° incidence angle, which corresponds to an attenuation in wave energy of 81% for the L = 1.48 cm (15.1 Hz) wave. Again we have inserted this value in Figure 6, and it can be seen that it is lower than the one received by wave staff measurements, but the difference is still within the experimental errors.

The Doppler measurements presented in Figure 5 (slick 3) show the spectra of the Doppler shift in areas *C*, *B*2, and *A* (see Figure 3*a*). The large decrease in spectral energy in the slick-covered areas is somewhat unexpected, but as is discussed in section 3*a*, this could be due to a directional dependence of the damping mechanism. The long waves propagate through area *C*, pass the slick areas *B*2 and *B*1, and then pass area *A*, as the velocity of the long waves is larger than the drift velocity of the slick. Thus the energy of the gravity waves should decrease as they propagate successively through the slick areas. After having passed the slick, wave energy again increases but is still smaller than it was in area *C*.

In Figure 8 we have plotted the ratios of the Doppler shift spectra for different areas. The low ratios for the lower frequencies could partly be caused by a shift of the spectral peaks in the slick areas. As is evident from the plot, the 90% confidence limits are very broad owing to the extremely short record time (here the confidence limits are even larger than in Figure 4, because the scatterometer several times lost phase lock and these time intervals had to be deleted when calculating the spectra).

b. Wind Wave Tank Experiments

The results of the wind wave tank experiments are summarized in Figures 9 and 10. Figure 9 shows that a direct influence by the oleyl alcohol surface film on wave damping is only discernable for frequencies $f \geq 2$ Hz. At 1 Hz (Figure 9*a*) a deviation from the logarithmic damping seems to occur in

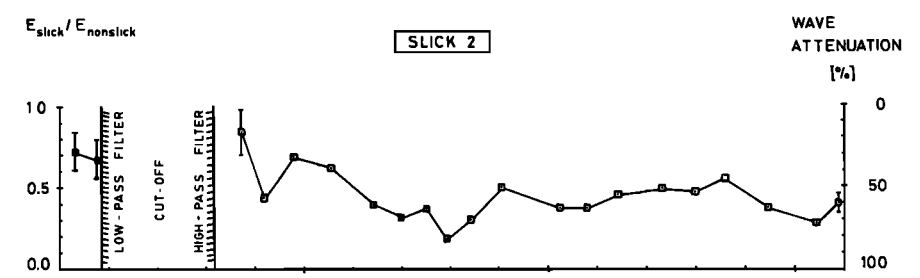

Fig. 7. Ratio of wave energy of slick area of slick 2 and nonslick area versus frequency measured by the vertical wave staff. The scale on the right-hand side shows the corresponding values for the wave attenuation in percent.

TABLE 2. Parameters Used for the Spectral Analysis of the Three Slick Experiments

	Record Time, s	Frequency Resolution, Hz	Degrees of Freedom	90% Confidence Limit for Ratio of Spectral Estimates
Slick 1				
wave staff	500	0.45	474	0.92/1.081
Slick 2				
wave staff	500	0.45	474	0.92/1.081
Slick 3				
scatterometer				
*B*1	243	0.36	64	0.75/1.26
*B*2	311	0.36	88	0.75/1.26
Slick 3				
wave staff				
B'1	149	0.45	144	0.82/1.18

both the slick and the nonslick case. But this is supposed to be an artifact due to an alteration of the water level in our wind wave tank at this specific frequency and fetch.

In order to clarify whether the above mentioned direct influence of the surface film can be described by the theory summarized by *Phillips* [1977] we calculated the γ_f/ω values (see section 2) from our wave tank data. The results, which are shown in Figure 10, seem to indicate that this theory, which was developed under the assumption of an inextensible film, does not apply for oleyl alcohol surface films. But it has to be stressed that damping coefficients γ_f/ω calculated from lower-frequency water waves ($f \leq 2$ Hz) are more sensitive to slope variations of the curves connecting the points in Figure 9 because of the low direct attenuation effect of oleyl alcohol films in this frequency range. In order to get more information on the damping mechanism of surface films, further investigations with different organic surface films are necessary.

5. Comparison With Theory

Whereas the wave damping of the capillary waves in the open ocean can be explained by a direct influence of the surface film, this does not hold for the lower-frequency gravity waves. The surface slick is supposed to modify not only the direct energy dissipation but also the wind input [*Barger et al.*, 1970] and the wave-wave interaction processes.

In order to separate these mechanisms and to gain insight into their frequency dependence and contribution to wave damping we performed first wave tank experiments with mechanically generated waves as described above. The result of these experiments is that the Phillips mechanisms cannot account for the observed higher γ_f/ω values. Additional dissipation by intermolecular interaction between the film-forming substances and the bulk water has to be postulated.

Since the wave tank data exclude a direct damping of water waves $f < 2$ Hz by an oleyl alcohol film, the observed gravity wave attenuation could be partly due to a decoupling between the wind field and the waves, as described by *Barger et al.* [1970]. But another important mechanism is the interaction between the different wave components. If short waves are damped by the surface film, then the wave-wave interaction mechanism can also lead to a damping of the longer waves. The observed damping rates are compatible with the assumption that an energy transfer from short to long waves occurs: in the presence of the surface film, about 40–60% of the energy in the short-wave spectrum is dissipated, which implies that less energy is available for a transfer to longer waves.

The question of the direction of energy transfer between short and long waves has been the subject of considerable debate: *Phillips* [1963] argued that the energy dissipated by the short waves had partly been acquired from long gravity waves, which would in total lead to a damping of long waves.

In contrast to this, *Longuet-Higgins* [1969] emphasized that as the short waves dissipate, they give up their momentum, thus exerting a horizontal stress. If short and long waves propagate in the same direction, this stress is in phase with the orbital velocity of the long waves, which should lead to their growth. A comparison between this effect and the mechanism proposed by *Phillips* [1963] shows that the energy input into the long-wave field is much greater than the energy loss due to Phillips' mechanism [*Longuet-Higgins*, 1969], assuming a steady regeneration of the short waves by the wind.

Apart from some arithmetical errors in Longuet-Higgins' model (K. Hasselmann, private communication, 1979), *Hasselmann* [1971] objected that the energy input to the long waves due to the rate of working of the effective surface stress exerted by dissipation of short waves is almost exactly balanced by the loss of potential energy arising from the mass transfer, the residual being just the original damping term discussed by *Phillips* [1963].

Garrett and Smith [1976] pointed out that a net long-wave growth can result if short-wave generation is correlated with the orbital velocity of the long waves. This effect was already included in *Hasselmann*'s [1971] analysis, but he assumed the correlation to be zero.

Some other authors [*Keller and Wright*, 1975; *Valenzuela and Wright*, 1976; *Snyder et al.*, 1977; *Shemdin*, 1977] have also recognized the potential importance of a correlation between short-wave generation and long-wave orbital velocity.

As a very intensive wave damping in the capillary wave range caused by oleyl alcohol slicks is proved in this work and in earlier publications [*Hühnerfuss et al.*, 1975, 1978], the regeneration of short waves is extremely hindered, so that a net gravity wave damping would be compatible with the model proposed by *Garrett and Smith* [1976] and with Hasselmann's mechanism, too, if the regeneration term is not considered to be zero.

However, further experiments have to be performed in order to exclude another possible effect on wave damping by surface films: after having damped a greater part of the energy in the capillary and short gravity wave range, wave-wave interaction processes could result in a redistribution of spectral energy within the wave spectrum, thus leading to wave damping of those spectral components on which no direct effect of the surface film is anticipated.

TABLE 3. Total Record Time and Relative Backscattered Power of the Four Areas *A*, *B*1, *B*2, and *C* (See Figure 3*a*) of Slick 3 Measured by the Tower Scatterometer

Area	Total Record Time, s	Relative Backscattered Power, dB
Slick-free area *A*	520	3.31 ± 0.43
Slick patch *B*1	32.5	9.66 ± 1.82
Slick patch *B*2	32.5	9.56 ± 2.22
Slick-free area *C*	520	3.60 ± 0.59

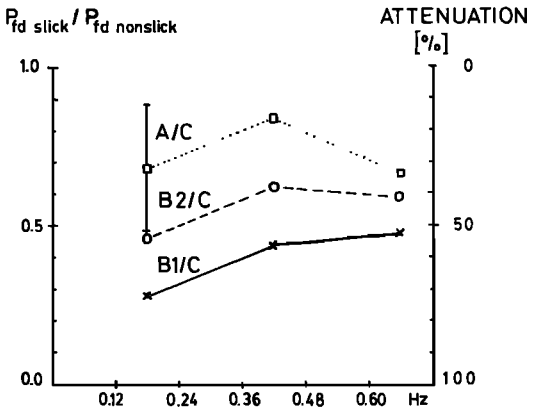

Fig. 8. Ratios of the Doppler spectra of areas *A*, *B*1, *B*2, and *C* of slick 3 (squares represent *A*/*C*, circles represent *B*2/*C*, and crosses represent *B*1/*C*).

6. Suggestions for Further Studies

A further confirmation of the above mentioned hypothesis on the energy transfer from short to long waves is expected by experiments in a wind wave tunnel: if the model described above is correct, a net wave damping should be observed if the short and long waves are propagating in opposite directions on a slick-free water surface. This is the case if the wind is blowing against plunger-generated long waves in a wind wave tunnel or against swell under natural conditions. If a slick is present under such experimental conditions, the wave damping in the gravity wave range should be less intensive than that with a clean water surface. According to suggestions of K. Hasselmann (private communication, 1979), the residual energy transfer leads to attenuation of the long waves, independent of their propagation direction to the short waves on a clean sea surface.

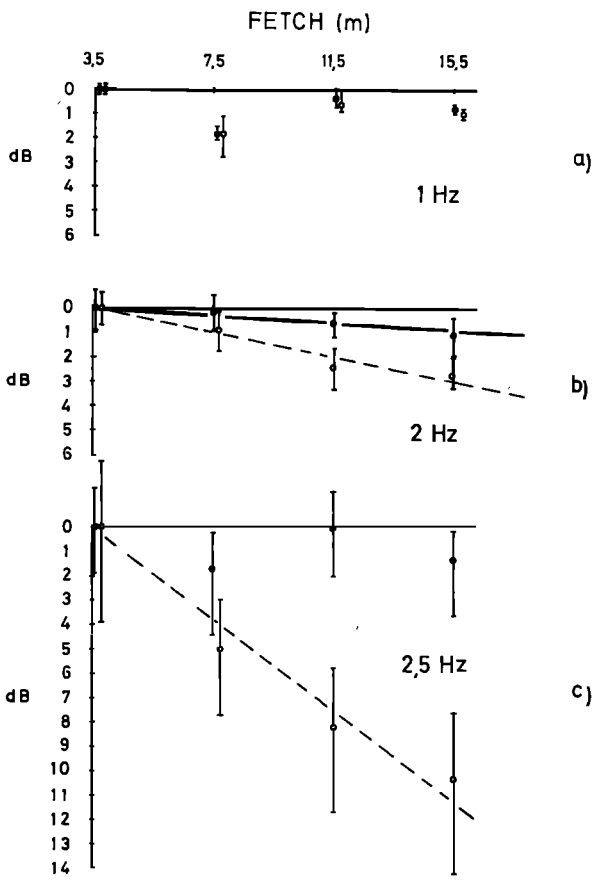

Fig. 9. Damping of mechanically generated 1-, 2-, and 2.5-Hz waves by an oleyl alcohol film (open circles) compared with a clean water surface (solid circles). The data points are averages of at least 500 waves.

The observed significant wave damping in the gravity wave range implies a decrease in the microwave backscattering cross section also for *L* band radars. For example, on Seasat SAR images (*L* band) many surface structures are discernable which might be explained by a nonuniform distribution of monomolecular surface films on the ocean surface, thus making internal waves, ocean fronts, current boundaries (Gulf Stream), and Langmuir cells visible by imaging radars. So there is an urgent need for simultaneous wave measurements by wave staffs and *L* band radars of slick-free and slick-covered ocean areas.

Wave attenuation rates in the presence of an oleyl alcohol surface film measured by *X* and K_u band radars seem to be higher than those received by conventional wave staffs. It is presumed that wave damping caused by surface films shows a directional dependence, which is differently resolved by wave staffs (omnidirectional) than by the relative received power of *X* and K_u band radar (unidirectional) or the spectra of the Doppler shift (directional dependent resolution). In order to confirm this hypothesis and thus improve the possibility for evaluation of radar data in the presence of natural slicks a careful investigation has to be performed to measure the wave attenuation rates with both wave staffs and radars looking in different directions on a slick-covered and slick-free sea surface.

7. Conclusions

1. In the presence of an oleyl alcohol surface film a wave attenuation of about 40–60% is observed in the frequency range between 3.2 and 16 Hz. A slight frequency dependence of the wave damping can be concluded from the slick experiments. Although the wave damping rates in the low-frequency

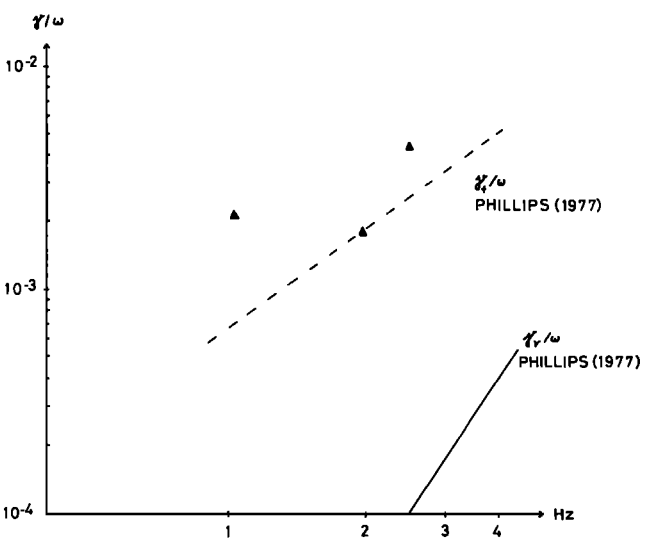

Fig. 10. Attenuation coefficient/frequency (γ/ω) plotted versus frequency of plunger-generated waves of a wave tank on a clean water surface (solid curve) and in the presence of an oleyl alcohol film (solid triangles). For comparison the theoretical curve for an inextensible film [after *Phillips*, 1977] is plotted (dashed curve).

part of the spectrum are less conclusive, the data seem to indicate that waves in the frequency range between 0.12 and 0.7 Hz are still subject to some damping.

2. From the measurements it is evident that the decrease of the L band radar cross section is expected to be almost as large as that for the K_u and the X band, since the wave damping is not very strongly dependent on frequency in the range from 3.2 to 16 Hz.

3. Wave tank experiments show that direct damping effects (viscous damping) of oleyl alcohol films are confined to a frequency range $f \geq 2$ Hz. The observed significant damping rates in the lower-frequency range can only be explained by indirect effects (modified wind input and modified wave-wave interaction). The observed damping of gravity waves by oleyl alcohol surface films is compatible with the assumption that energy is transferred from short to long waves. The nondimensional γ_f/ω values, calculated from the wave tank data, indicate a contribution of intermolecular interaction between film-forming substances and the bulk water to damping of water waves by surface films.

APPENDIX X

The Doppler shift f_d is given by the velocity of the illuminated patch in the look direction of the antenna:

$$2\pi f_d = 2\mathbf{K} \cdot \mathbf{U} \tag{A1}$$

where $\mathbf{K}$ is the wave number of the incident microwave radiation and $\mathbf{U}$ the orbital velocity. If we write the surface elevation ζ and the orbital velocity $\mathbf{U}$ associated with the long ocean waves as Fourier integrals

$$\zeta = \int z(\mathbf{k})e^{i(\mathbf{k}x-\omega t)} + \text{c.c.})\, d\mathbf{k} \tag{A2}$$

$$\mathbf{U} = \int \mathbf{u}(\mathbf{k})e^{i(\mathbf{k}x-\omega t)} + \text{c.c.})\, d\mathbf{k} \tag{A3}$$

where c.c. stands for complex conjugate, then the components of $\mathbf{u}(\mathbf{k})$ are given by [see *Kinsman*, 1965]

$$\begin{aligned} u_x(\mathbf{k}) &= \omega(k_x/|\mathbf{k}|)z(\mathbf{k}) \\ u_y(\mathbf{k}) &= \omega(k_y/|\mathbf{k}|)z(\mathbf{k}) \\ u_z(\mathbf{k}) &= -i\omega z(\mathbf{k}) \end{aligned} \tag{A4}$$

The surface elevation spectrum of the long waves, $P_\zeta(\mathbf{k})$, is defined by

$$\langle z(\mathbf{k})z^*(\mathbf{k}')\rangle = \tfrac{1}{2}\delta(\mathbf{k}-\mathbf{k}')P_\zeta(\mathbf{k})\rangle \tag{A5}$$

and the Doppler spectrum $P_{f_d}(\mathbf{k})$ by

$$\frac{1}{(2\pi)^2}\langle 2\mathbf{K}\cdot\mathbf{u}(\mathbf{k})[2\mathbf{K}\cdot\mathbf{u}(\mathbf{k})]^*\rangle = \tfrac{1}{2}\delta(\mathbf{k}-\mathbf{k}')P_{f_d}(\mathbf{k}) \tag{A6}$$

where angle brackets denote the ensemble average, δ the Dirac delta function, and the asterisk, complex conjugation. If we express $\mathbf{k}$ and $\mathbf{K}$ in terms of their modulus, the azimuth angle ϕ, and the incidence angle θ, we obtain

$$(\mathbf{K}\cdot\mathbf{u})(\mathbf{K}\cdot\mathbf{u})^* = |\mathbf{K}|^2\omega^2(\sin^2\theta\cos^2\phi + \cos^2\theta)\cdot z(\mathbf{k})z^*(\mathbf{k}') \tag{A7}$$

Inserting this expression in (A6) and comparing it with (A5) yield the result

$$P_{f_d}(\mathbf{k}) = |\mathbf{K}|^2(\omega/\pi)^2[\sin^2\theta\cos^2\phi + \cos^2\theta]P_\zeta(\mathbf{k})$$

Acknowledgments. This research has been sponsored by the Deutsche Forschungsgemeinschaft (German Science Foundation) through the Sonderforschungsbereich 94, Meeresforschung, Hamburg. The authors wish to thank Henkel & Cie GmbH, Düsseldorf, which generously provided the slick material (oleyl alcohol) at no cost; H. Dannhauer, who prepared the frozen chunks during the experiments; J. Meier for his help during data evaluation and spectral analysis; and F. Feindt for his assistance during the wave tank experiments. Our thanks are due the Jonswap scientists for gathering the data and for stimulating discussions, especially K. Hasselmann for several enlightening critical remarks.

REFERENCES

Adam, N. K., A rapid method for determining the lowering of tension of exposed water surfaces, with some observations on the surface tension of the sea and inland waters, *Proc. R. Soc. London, Ser. B, 122,* 134–139, 1937.

Au, B., J. Kenney, L. U. Martin, and D. Ross, Multi-frequency radiometric measurements of foam and a monomolecular slick, *Proc. Int. Symp. Remote Sensing Environ. 9th, 1,* 1763–1773, 1974.

Barger, W. R., W. D. Garrett, E. L. Mollo-Christensen, and K. W. Ruggles, Effects of an artificial sea slick upon the atmosphere and the ocean, *J. Appl. Meteorol., 9,* 396–400, 1970.

Barger, W. R., W. H. Daniel, and W. D. Garrett, Surface chemical properties of banded sea slicks, *Deep Sea Res., 21,* 83–89, 1974.

Bendure, R. L., and R. S. Hansen, Capillary ripple investigations on monolayers at intermediate elasticities, *J. Phys. Chem., 71,* 2889–2892, 1967.

Brockmann, U. H., G. Kattner, G. Hentzschel, K. Wandschneider, H. D. Junge, and H. Hühnerfuss, Natürliche Oberflächenfilme in Seegebiet vor Sylt, *Mar. Biol. Berlin, 36,* 135–146, 1976.

Broecker, H.-C., J. Petermann, and W. Siems, The influence of wind on CO_2-exchange in a wind-wave tunnel, including the effects of monolayers, *J. Mar. Res., 36,* 595–610, 1978.

Cox, C., and W. Munk, Some problems in optical oceanography, *J. Mar. Res., 14,* 63–78, 1955.

Davies, J. T., and E. K. Rideal, *Interfacial Phenomena,* 479 pp., Academic, New York, 1963.

Drost-Hansen, W., Molecular aspects of aqueous interfacial structures, *J. Geophys. Res., 77,* 5132–5146, 1972.

Garrett, C., and J. Smith, On the interaction between long and short surface waves, *J. Phys. Oceanogr., 6,* 925–930, 1976.

Garrett, W. D., Damping of capillary waves at the air-sea interface by oceanic surface-active material, *J. Mar. Res., 25,* 279–291, 1967.

Garrett, W. D., and W. A. Zisman, Damping of capillary waves on water by monomolecular films of linear polyorganosiloxanes, *J. Phys. Chem., 74,* 1796–1805, 1970.

Goodrich, F. C., The mathematical theory of capillarity, II, *Proc. R. Soc. London, Ser. A, 260,* 490–502, 1961.

Goodrich, F. C., On the damping of water waves by monomolecular films, *J. Phys. Chem., 66,* 1858–1863, 1962.

Gottifredi, J. C., and G. J. Jameson, The suppression of wind-generated waves by a surface film, *J. Fluid Mech., 32,* 609–618, 1968.

Hasselmann, K., On the mass and momentum transfer between short gravity waves and larger-scale motions, *J. Fluid Mech., 50,* 189–205, 1971.

Hasselmann, K., et al., Measurements of wind-wave growth and swell decay during the Joint North Sea Wave Project (Jonswap), *Dtsch. Hydrogr. Z., Suppl. A, 8*(12), 95 pp., 1973.

Horne, R. A., Structure of seawater and its role in chemical mass transport between the sea and the atmosphere, *J. Geophys. Res., 77,* 5170–5175, 1972.

Hühnerfuss, H., and P. Lange, Modification of air sea interaction processes, I, A new method for producing artificial sea slicks, *Rep. 7,* pp. 163–169, Sonderforschungsbereich 94, Univ. of Hamburg, Hamburg, 1975.

Hühnerfuss, H., W. Walter, P. A. Lange, J. Teichert, and H. J. Vollmers, Modification of air-sea interaction processes by artificial slicks, *Proc. IAHR Congr. 16th, 3,* 509–515, 1975.

Hühnerfuss, H., P. Lange, J. Teichert, and H. Vollmers, A wind wave tunnel for the investigation of artificial slick wave damping and drift, *Meerestech. Mar. Tech., 7,* 23–26, 1976.

Hühnerfuss, H., W. Walter, and G. Kruspe, On the variability of surface tension with mean wind speed, *J. Phys. Oceanogr., 7,* 567–571, 1977.

Hühnerfuss, H., W. Alpers, and W. L. Jones, Measurements at 13.9 GHz of the radar backscattering cross section of the North Sea covered with an artificial surface film, *Radio Sci., 13,* 979–983, 1978.

Jones, W. L., F. J. Wentz, and L. C. Schroeder, Algorithm for infer-

ring wind stress from Seasat-A, *J. Spacecr. Rockets, 15*(6), 368–374, 1978.

Keller, W. C., and J. W. Wright, Microwave scattering and the straining of wind-generated waves, *Radio Sci., 10,* 139–147, 1975.

Keller, W. C., and J. W. Wright, Modulation of microwave backscatter by gravity waves in a wave tank, *Rep. 7968,* Nav. Res. Lab., Washington, D. C., 1976.

Kinsman, B., Wind waves: Their generation and propagation on the ocean surface, 676 pp., Prentice-Hall, Englewood Cliffs, N. J., 1965.

Lange, P., and H. Hühnerfuss, Drift response of monomolecular slicks to wave and wind action, *J. Phys. Oceanogr., 8,* 142–150, 1978.

Longuet-Higgins, M. S., A nonlinear mechanism for the generation of sea waves, *Proc. R. Soc. London, Ser. A, 311,* 371–389, 1969.

Lucassen, J., and R. S. Hansen, Damping of waves on monolayer-covered surfaces, I, Systems with negligible surface dilational viscosity, *J. Colloid Interface Sci., 22,* 32–44, 1966.

Mallinger, W. D., and T. P. Mickelson, Experiments with monomolecular films on the surface of the open sea, *J. Phys. Oceanogr., 3,* 328–336, 1973.

Phillips, O. M., On the attenuation of long gravity waves by short breaking waves, *J. Fluid Mech., 16,* 321–332, 1963.

Phillips, O. M., *The Dynamics of the Upper Ocean,* 2nd ed., 336 pp., Cambridge University Press, New York, 1977.

Plinius, C., Secundus, *Historia Naturalis,* book 2, chap. 103, 77 A.D.

Shemdin, O. H., Modulation of centimetric waves by long gravity waves: Progress report on field and laboratory results, in *Proceedings of the Nato Symposium on Turbulent Fluxes Through the Sea Surface: Wave Dynamics and Prediction, Marseilles, September 12-16,* pp. 235–255, Plenum, New York, 1977.

Snyder, R. L., R. B. Long, F. W. Dobson, and J. A. Elliot, The Bight of Abaco Pressure Experiment, in *Proceedings of the Nato Symposium on Turbulent Fluxes Through the Sea Surface: Wave Dynamics and Prediction, Bendor, France,* pp. 433–443, Plenum, New York, 1977.

Tober, G., R. C. Anderson, and O. H. Shemdin, Laser instrument for detecting water ripple slopes, *Appl. Opt., 12,* 788–794, 1973.

Valenzuela, G. R., and J. W. Wright, The growth of waves by modulated wind stress, *J. Geophys. Res., 81,* 5795–5796, 1976.

Valenzuela, G. R., M. B. Laing, and J. C. Daley, Ocean spectra for the high frequency waves from airborne radar measurements, *J. Mar. Res., 29,* 69–84, 1971.

van den Tempel, M., and R. P. van de Riet, Damping of waves by surface-active materials, *J. Chem. Phys., 42,* 2769–2777, 1965.

Vollhardt, D., and R. Wüstneck, Untersuchungen über das dynamische Verhalten gespreiteter Monoschichten an der Grenzfläche Luft/wässriger Lösung, III, Oberflächenpotentialuntersuchungen an gemischten gespreiteten Monoschichten von Na-n-Octadecylsulfat und n-Octadecanol, *Colloid Polymer Sci., 256,* 1095–1101, 1978.

Wentz, F., and W. L. Jones, Description of computer program TWRSCAT: Generation of time series for the Pisa tower wavestaffs and scatterometer measurements, *Tech. Rep. FWA 76-001,* 28 pp., NASA Langley Res. Cent., Hampton, Va., 1976.

Wright, J. W., Backscattering from capillary waves with application to sea clutter, *IEEE Trans. Antennas Propag., AP-14,* 749–754, 1966.

Wright, J. W., A new model for sea clutter, *IEEE Trans. Antennas Propag., AP-16,* 217–223, 1968.

(Received December 26, 1979;
revised June 9, 1980;
accepted June 10, 1980.)